 doi:10.20944/preprints202105.0173.v1

Article

Monitoring of the environmental corrosivity in museums by RFID sensors: application to pollution emitted by archeological woods

S. Rioual [1,*], B. Lescop [1], J. Pellé [1], G. De Alkmim Radicchi [2], G. Chaumat [2], M.D. Bruni [2], J. Becker [3] and D. Thierry [3]

[1] Univ Brest, Lab-STICC, CNRS, UMR 6285, F-29200 Brest, France ; rioual@univ-brest.fr; benoit.lescop@univ-brest.fr; julien.pelle@univ-brest.fr
[2] ARC-Nucléart, CEA-Grenoble, 17 rue des Martyrs, 38054 Grenoble, France; gilles.chaumat@cea.fr; gerusa.dealkmimradicchi@cea.fr; Marie-Dominique.bruni@cea.fr
[3] Institut de la Corrosion, 220 rue Pierre Rivoalon, 29200 Brest, France ; johan.becker@institut-corrosion.fr; dominique.thierry@institut-corrosion.fr
* Correspondence: rioual@univ-brest.fr

Abstract: The control of air quality in museums or storages is of fundamental interest for the conservation of historic artifacts. The present work reports an example of application of RFID sensors developed in the European project SensMat and dedicated to this issue. The sensors are based on the variation of property of an RFID tag coupled to a sensitive silver thin film exposed to the environment. As it will be described in the paper, such low cost sensors are interrogated by a commercial reader and provide the environmental corrosivity index and thus the presence of pollutants. The selected case study concerns the monitoring of pollution by H_2S in a building dedicated to conservation and restoration of archeological and historical woods. The ability of sensors to map spatially the corrosivity within buildings is highlighted.

Keywords: environmental corrosivity; air quality; IOT; autonomous sensor; RFID; corrosion; archeological wood

1. Introduction

Air pollution monitoring is of crucial interest for conservation and protection of historical artifacts in indoor environments. Indeed, gaseous pollutants in air are responsible of the degradation of many types of objects and materials. They are of diverse nature (organic acids, H_2S, NH_3, SO_2, NO_2 …) and are produced either internally in the building where are localized artifacts or externally due to outdoor pollution [1]. Some devices dedicated to the monitoring of air quality exist and may be applied for cultural heritage conservation. These include the use of sampling techniques or gas sensors. An alternative to these methods is to consider the chemical reactivity of metallic surfaces. In this case, all synergic parameters including the pollutants, temperature and humidity are taken into account. The measurement of the quantity of corrosion products at the surface as well as the mass loss of metal is then an indicator environmental corrosivity and allows evaluating the risk to the objects' integrity. For indoor applications, the ISO 11844-1 standard [2] gives the IC corrosivity classes which range from IC1 (very low corrosivity) to IC5 (very high corrosivity). Steel, zinc, copper and silver are sensitive to different pollutants and are therefore selected in this standard.

Electrical resistance (ER) is a well-established method to provide the IC class. In particular, the AirCorr™ sensor was commercialized within a project supported by the

 doi:10.20944/preprints202105.0173.v1

European Commission (Protection of cultural heritage by real-time corrosion monitoring) and dedicated to the monitoring of corrosive atmospheres in the cultural heritage sector [3-5]. In this case, the sensitive part the sensor is constituted by a strip elaborated in copper or silver. From the change in geometry of this metallic element (*i.e.*, thinning) induced by corrosion, it is possible to calculate the loss of metal thickness and hence the corrosivity class IC.

During the last decades, Radio-Frequency Identification (RFID) technology has become more and more popular in many industries and for a variety of applications including the cultural heritage sector [6,7]. It is indeed an efficient way to transfer data and track items. This attractiveness is explained by the ability of this technology to interrogate numerous tags at a very low price and with a low visual nuisance. Recently, RFID sensors were proposed for corrosion monitoring [8-19]. Within the European project SensMat, an UHF-RFID corrosion sensor was in particular developed to assess air quality and IC classes in museums [19]. It was subsequently applied for civil engineering applications [20]. As for ER sensors, the change of electrical resistance of a thin metallic film induced by corrosion is used to provide information on the environmental corrosivity. Due to its very low cost, this type of sensor is affordable for all museums including small ones and can be deployed at large scale.

The present study aims at demonstrating the interest of such sensors for monitoring the presence of air pollutants in buildings dedicated to cultural heritage such as museums, storages,…. This was performed at the ARC-Nucleart institute, which is specialized in conservation-restoration of archeological and historical woods. Archeological woods undergo a conservation treatment in the workshop by conventional chemical treatments based on polyethylene glycol (PEG). However, for large structures such as ships, this process does not exclude the formation of acidic iron species at the surface [21, 22]. These latter are known to generate H_2S pollution in the atmosphere and may affect other historical objects present in the building such as metals, pigments,…. Within this context, monitoring corrosivity of several areas in the building is of crucial interest. The present work describes first the buildings under monitoring and in more details the selected areas. The principle of RFID sensors which are based on the chemical reactivity of silver thin films is then presented. The results achieved by the sensors highlight clearly that the degree of pollution by H_2S is restricted to some area. In particular, due to the HVAC equipment, the laboratory used for restoration of polychromatic woods presents a low or very low corrosivity index with respect to storage rooms where acidification of archeological woods is an issue for conservation. These results are supported by data obtained by chemical analysis of sensitive thin films after exposure.

2. Materials and Methods

Due to the strong reactivity of silver surfaces to sulphide, silver thin films are considered in the present work. They were deposited on polycarbonate substrates (2.0 x 8.5 cm^2) by radio-frequency magnetron sputtering (Univex 350, Oerlikon). For sputtering deposition, the working chamber was vacuumed to reach a base pressure of 3×10^{-7} mbar. The substrate was fixed at a distance of ca. 8 cm parallel to the Ag target surface (diameter: 3 inches). Films were deposited for 30 seconds in Argon plasma. The Argon purity was

Preprints (www.preprints.org) | NOT PEER-REVIEWED | Posted: 10 May 2021 doi:10.20944/preprints202105.0173.v1

99.999 %. During deposition, the pressure was kept at 7×10^{-3} mbar. The input power at the target was 100 W. The resulting layers were ca. 20 nm thick. X-ray diffraction (XRD) was done to analyze the crystalline structure of the Ag layers using PANalytical Empyrean apparatus with CuK radiation (1.5408 Å).

3. Results

3.1. Description of areas under monitoring

The influence of archeological wood on the air quality was studied in two buildings. The maps of the buildings are presented in Fig. 1. The localizations of archeological materials containing pyrite (FeS_2) are indicated in the maps by blue stars.

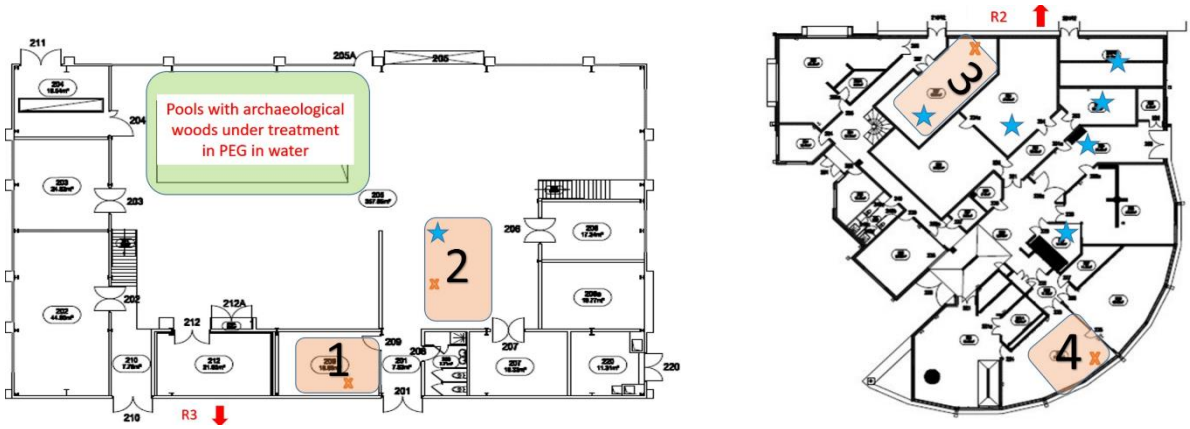

(**a**) (**b**)

Figure 1. (**a**) Description of the first building; (**b**) Description of the second building. Locations of archeological wood are indicated by blue stars.

Such archeological objects are considered to be the main source of pollution by H_2S. Indeed, pyrite oxidises naturally following the reaction [23-26] :

$$FeS_2 + H_2O + \frac{7}{2}O_2 \rightarrow Fe^{2+} + 2SO_4^{2-} + 2H^+ \quad (1)$$

After this step, the oxidation of Fe(II) can occurs to form Fe(III) which can then, *a priori*, oxidise FeS_2 at a much higher rate than oxygen.

$$2Fe^{2+} + \frac{1}{2}O_2 + 2H^+ \rightarrow 2Fe^{3+} + H_2O \quad (2)$$

$$FeS_2 + 14Fe^{3+} + 8H_2O \rightarrow 15Fe^{2+} + 2SO_4^{2-} + 16H^+ \quad (3)$$

The main consequence of this is the significant formation of protons which induce H_2S pollution by reaction of this extreme acidity on pyrite itself.

Due to the localisation of objects containing pyrite in the buildings, some areas were selected for the monitoring of the pollution. As seen in Fig. 1(a), two monitored spaces are in the first building: the biochemistry laboratory (space 1) and the temporary storage area for archaeological artefacts (space 2). Two locations are also selected in the second building where most of the objects are stored: the storage area for archaeological artefacts (space 3) and the sculpture workshop (space 4). The sources of H_2S are in storage areas

Preprints (www.preprints.org) | NOT PEER-REVIEWED | Posted: 10 May 2021 doi:10.20944/preprints202105.0173.v1

(spaces 2 and 3). Monitoring the two other locations will provide information on the environmental corrosivity of nearby areas with (space 4) and without HVAC (space 1).

Figure 2 displays pictures of the monitored areas in the first building which is dedicated to the reception of archaeological artifacts and to their treatment by PEG. The entrance hall is shown in Fig. 2(a). In this large open space area, archeological wood treatment pools can be seen. A big shed displayed in Fig. 2(b) is also present and serves as temporary storage room for archaeological artefacts. Materials stored in this place are: wood, leather, vegetal fibers, and metals. The environmental corrosivity inside the shed was monitored due to the presence of potential sources of H_2S (space 2). Indeed, as seen in Fig. 2(c), a large plastic package containing a treated archeological basket with sediments and a treated boat placed on the metallic support are stored at this location. In the first building, to evaluate the air quality in other rooms, the biochemistry laboratory (space 1) was also selected. It is separated by only few meters from the shed. In this room, no archeological wood are stored. Fig. 2(d) displays a picture of this area.

Figures 3 display pictures of the spaces under monitoring in the second building. This latter concentrates the majority of restoration workshops and storage of archeological and historical collections. The archaeological storage area (space 3) is depicted in Fig. 3(a) and stores wooden after their resin/drying treatment. Some integrated metal in very small proportion are also there. The wood comes from boats at different historical periods, from Romans to Modern. The HVAC keeps the temperature and relative humidity constant at 22°C and 45% RH.

The sculpture restoration workshop (space 4) is shown in Fig. 3(b). In this area, activities of conservation-restoration for historical polychromatic wood are performed. Medieval, Renaissance and Early modern polychrome religious sculptures are the main objects restored in the Workshop. These polychromes are generally produced by metallic coatings (silver or gold) and coloured pigments (metallic carbonates or acetates). Pollution by H_2S is a problem for such type of collection because this pollutant is known to react with metals even at very low concentrations leading to tarnishing surfaces and also with pigments, causing darkening of the polychromy [27,28,29,30]. To limit such effects, the HVAC of the room keeps the temperature and relative humidity relatively constant and below 25° C and 60% RH. Checking the low corrosivity in this space by the proposed method is a key point of the present study.

(**a**)

(**b**)

Preprints (www.preprints.org) | NOT PEER-REVIEWED | Posted: 10 May 2021 doi:10.20944/preprints202105.0173.v1

(**c**) (**d**)

Figure 2. (**a**) Entrance hall for treatment of woods; (**b, c**) The shed used for temporary storage area (space 2); (**d**) The biochemistry laboratory (space 1).

(**a**) (**b**)

Figure 3. (**a**) Storage room for archeological woods (space 3); (**b**) Sculpture restoration workshops (space 4).

3.2. Description of the sensor

The RFID sensor is presented in Fig. 4(a). Its dimension are 11.3 x 6.5 cm^2. The principle of the sensor was described in details in Refs. [19,20]. It is based on the electromagnetic coupling between a metallic sensitive layer exposed to a corrosive environment and the antenna of an RFID tag. The sensitive layer is shown in Fig. 4(a). It is interacting with the RFID tag ALN-9654 "G" from Alien technologies which is localized under the white plastic film. Corrosion of this active layer induces an increase of its electrical resistance and hence, a change of the property of the coupled antenna. The signal strength emitted from the tag to the reader is then modified. This variation can be monitored by measuring the RSSI (Received Signal Strength Indication) by a commercial UHF-RFID reader. Due to this operating principle, the sensor in its initial state *i.e.* before corrosion does not respond to the reader. This problem is solved by considering a second RFID tag which serves as a reference for the device. It is represented by dotted line in Fig. 4(a). Fig. 4(a) displays the UHF-RFID reader used for the interrogation of the sensor. The portable CS108 model from Convergence Systems Limited was chosen. As shown, a mobile phone is connected by Bluetooth to the reader. The RSSI value and identification number associated with the two tags appears then on the mobile.

Preprints (www.preprints.org) | NOT PEER-REVIEWED | Posted: 10 May 2021 doi:10.20944/preprints202105.0173.v1

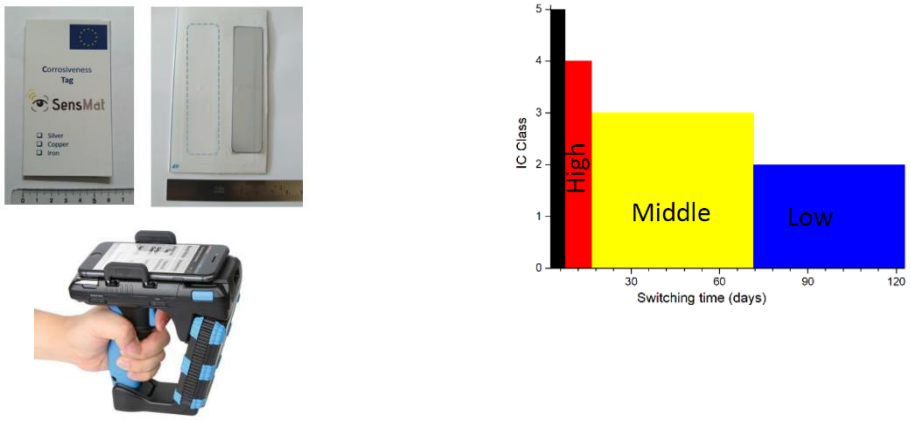

(**a**) (**b**)

Figure 4. (**a**) The two sides of the sensor and the UHF-RFID reader; (**b**) The relation between the IC class and the detection time of the sensitive tag.

In the present work, silver thin films are used since this metal is known to be sensitive to H_2S [31]. To present the method, sensors produced by silver thin films of different thicknesses are considered. Table 1 reports the data for the interrogation of the sensors by maintaining a distance of 40 cm between the reader and the sensor.

Table 1. RSSI values for the reference and sensitive RFID tags for several values of the silver thickness films. The electrical resistance of the thin films are also given.

Thickness (nm)	RSSI Reference (dBm)	RSSI Sensitive (dBm)	Electrical Resistance (Ω)
20	-45	No detection	14
10	-45	No detection	43
7.5	-45	-55	82
5	-45.5	-49	300

As seen, the reference tag is detected with a RSSI value of -45 dBm, independently of the thickness of the sensitive layer. Concerning the sensitive tag, it can be detected only when a metallic film of 7.5 nm thickness or less is present. For this thickness threshold value of 7.5 nm, the difference between the two RSSI values is about 10 dB. Decreasing the thickness of silver to 5 nm reduces this difference to 4 dBm. As shown in the table, the observed behavior is explained by the increase of the electrical resistance of the sensitive film. This variation of the electrical resistance does not depends linearly on the thickness, a result in agreement with numerous studies made on thin films. The value of the electrical resistivity also deviates from the electrical conductivity of bulk materials. These results achieved on thin films can be applied to corrosion monitoring since, by assuming an uniform corrosion process, corrosion also leads to a regular loss of thickness. The detection of the sensitive tag is associated to a decrease of the metallic thickness below the threshold value of 7.5 nm. By producing thin films with an initial thickness of 20 nm, the exposure time necessary to observe the tag can therefore be used to extract the different IC classes. Fig. 4(b) displays the relation between this switching time and the different IC classes. As seen, if the sensitive tag is observed before 15 days of exposure, the IC class is IC5 or IC4. An IC3 class (middle corrosivity) is achieved if this transition occurs between 16 and 71 days of exposure.

Preprints (www.preprints.org) | NOT PEER-REVIEWED | Posted: 10 May 2021 doi:10.20944/preprints202105.0173.v1

3.2. Corrosivity classes at different locations

The sensors were interrogated each weeks from December 15th 2020 to March 15th 2021. Fig. 5(a) reports the exposure time needed to recover the signal from the sensitive tag. As observed, important differences exist between the different areas under monitoring. Indeed, the loss of 12.5 nm of metal thickness was achieved in the biochemistry laboratory (space 1) in 36 days. This time increases for the two storages rooms (spaces 2 and 3) to 50 and 57 days. The observation of the sensitive tag was never realized for the culture restoration workhop (space 4). The time needed to detect the sensitive tag is directly associated with the environmental corrosivity. Results achieved for the space 2 and 3 are similar. In this two cases, the non negligible corrosivity is explained by the presence of numerous archeological woods in these storage areas and therefore some emission of H_2S. In contrast, a very limited corrosion effect is measured in space 4 where polychromatic woods are restored. The absence of corrosion is then certainly due to the use of HVAC in the building. The higher corrosion rate observed in space 1 is rather surprising. It is indeed the worst case while no source of pollution emission is expected in this area.

Location	Detection time (days)
Space 1	36
Space 2	57
Space 3	50
Space 4	>95

(**a**)

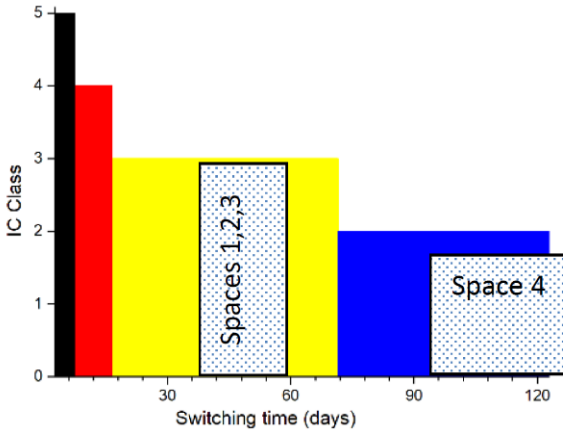

(**b**)

Figure 5. (**a**) Reporting of the detection time for the sensitive tag for the different areas under monitoring; (**b**) IC class for the different spaces.

As explained above, the IC index can be calculated from the time of detection. Fig 5(b) present the index for the different locations. Middle corrosivity class (IC3) is measured for the space 1, 2 and 3. Space 4 presents a low corrosivity (IC2) or very low corrosivity (IC1) level.

To further get some insight on the results provided by sensors, the four sensitive metallic films were analyzed after their exposure by conventional analytical methods. Fig. 6 displays the XRD patterns of the silver thin films.

Preprints (www.preprints.org) | NOT PEER-REVIEWED | Posted: 10 May 2021 doi:10.20944/preprints202105.0173.v1

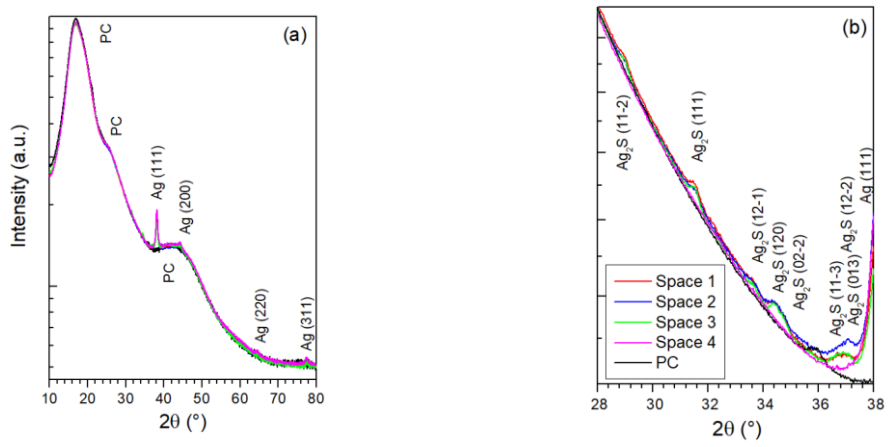

(**a**) (**b**)

Figure 6. (**a**) XRD diffractograms of exposed silver samples and polycarbonate substrate; (**b**) XRD patterns between 28° and 38°.

The characterization of the uncoated polycarbonate substrate is also presented as a reference. Fig. 6(a) shows the patterns in the range from 10° to 80°. The broad structures observed at 17°, 26° and 42° are attributed to the polycarbonate substrate. The peak corresponding to metallic silver Ag(111) appears at about 38° for all sample. The highest intensity of this peak is obtained on the sample exposed in space 4, indicating that a higher metal thickness remains for this sample. This result is in agreement with the low IC index of this area measured by the sensor. To characterize more precisely the possible corrosion products, additional measurements were done from 28° to 38°. They are presented in Fig. 6(b). Several peaks are clearly visible on samples exposed in spaces 1, 2 and 3 but not in space 4. They are assigned to Acanthite Ag_2S, which presents a monoclinic structure [32]. Studies focusing on reactivity of silver to H_2S are frequently reported in the literature [33-37]. The sulfidation process may occur via different pathways but leads always to the formation of Ag_2S on the surface, in agreement with our findings. From this result, it appears clearly that the high corrosivity of space 1 is also associated to sulfidation even if no source of emission are present in the room. The higher corrosion rate achieved in this area may be explained by the presence of sources in the vicinity (space 2, for example) and by the presence of other contaminants in this area.

5. Conclusions

As a conclusion, the present work reports the application of corrosion RFID sensors produced with silver thin films for the monitoring of H_2S pollution in buildings dedicated to conservation and restoration of woods. The sensor can be considered as a binary sensor (True/False) based on the detection of a sensitive tag due to a loss of metal induced by corrosion. From the detection of the threshold value, it is possible to define the index of environmental corrosivity of the monitored area and hence to provide a map of corrosivity of the buildings. The sensitivity of the sensor is a tunable parameter since it depends on the nature of the selected metal and on its initial thickness. Silver films with 20 nm thickness were chosen here to probe the IC3/IC2 categories with few months of exposure. The achieved results highlight the important role of HVAC to reduce the corrosivity level

 doi:10.20944/preprints202105.0173.v1

in the sculpture restoration workshop with respect to storage areas. The proposed method can be extended to many issues in museums or storage areas, and should therefore be considered as a promising one within the concept of preventive conservation for cultural heritage.

Funding: This work received funding from the European Union's Horizon H2020 research and innovation program under grant agreement 814596 (Preventive solutions for Sensitive Materials of Cultural Heritage – SENSMAT).

Author Contributions: For research articles with several authors, a short paragraph specifying their individual contributions must be provided. The following statements should be used "methodology, S.R., B.L., G.C., G.D.A.R, M.D.B., J.B., D.T.; validation, S.R., B.L., J.P. G.C., G.D.A.R, M.D.B., J.B., D.T.; investigation, S.R., B.L., J.P., G.C., J.B.; visualization, S.R., G.D.A.R., writing—original draft preparation, S.R.; writing—review and editing, S.R., B.L., J.P., G.C., G.D.A.R, M.D.B., J.B., D.T.; project administration, S.R., G.C., M.D.B., D.T.; All authors have read and agreed to the published version of the manuscript." Please turn to the CRediT taxonomy for the term explanation. Authorship must be limited to those who have contributed substantially to the work reported.

Conflicts of Interest: Declare conflicts of interest or state "The authors declare no conflict of interest." Authors must identify and declare any personal circumstances or interest that may be perceived as inappropriately influencing the representation or interpretation of reported research results. Any role of the funders in the design of the study; in the collection, analyses or interpretation of data; in the writing of the manuscript, or in the decision to publish the results must be declared in this section. If there is no role, please state "The funders had no role in the design of the study; in the collection, analyses, or interpretation of data; in the writing of the manuscript, or in the decision to publish the results".

References

1 Fish, P.; Muller, C.; Thickett, D. An air quality standard for the protection of cultural heritage. *Papyrus* **2014**, 15(2): 26-29

2 ISO 11844-1, Corrosion of metals and alloys – classification of low corrosivity of indoor atmospheres – Part 1: determination and estimation of indoor corrosivity. International Organization of Standardization, Genève, Suisse, **2006.**

3 Kouril, M.; Prosek, T.; Scheffel, B.; Dubois, F. High sensitivity electrical resistance sensors for indoor corrosion monitoring. *Corrosion Engineering Science and Technology* **2013**, 48, pp. 282–287.

4 Kouril, M.; Prosek, T.; Scheffel, B.; Degres, Y. Corrosion monitoring in archives by the electrical resistance technique. *Journal of Cultural Heritage* **2014**, 15, pp. 99–103.

5 Prosek, T.; Taube, M.; Dubois, F.; Thierry, D. Application of automated electrical resistance sensors for measurement of corrosion rate of copper, bronze and iron in model indoor atmospheres containing short-chain volatile carboxylic acids. *Corrosion Science* **2014**, 87, pp. 376–382.

6 Ciofi, L.; Zappia, I.; Balleri, R.; Gherardelli, M. RFID applied to the cataloguing of a collection of historical plaster moulds. *Journal of Cultural Heritage* **2016**, 21, pp. 910-914.

7 Giuliano, R.; Mazzenga, F.; Petracca, M.; Vatalaro, F. Application of Radio Frequency Identification for Museum Environment. *Enabling Technologies: Infrastructure for Collaborative Enterprises (WETICE) 2013 IEEE 22nd International Workshop* **2013**, pp. 190-195.

8 Zarifi, M.; Deif, S.; Abdolrazzaghi, M.; Chen, B.; Ramsawak, D.; Amyotte, M.; Vahabisani, N.; Hashisho, Z.; Chen, W.; Daneshmand, M. A microwave ring resonator sensor for early detection of breaches in pipeline coatings. *IEEE Transactions on industrial electronics* **2017**, 65, pp. 1626-1635.

9 Zarifi, M.; Deif, S.; Daneshmand, M.; Wireless passive RFID sensor for pipeline integrity monitoring. *Sensors and Actuators A: Physical* **2017**, 261, pp. 24-29.

10 Deif, S.; Daneshmand, M. Long array of microwave sensors for real-time coating defect detection. *IEEE Transactions on Microwave Theory and Techniques* **2020**, 68, pp. 2856-2866.

11 Deif, S.; Daneshmand, M. Multiresonant chipless RFID Array System for Coating Defect Detection and Corrosion prediction *IEEE Transactions on industrial electronics* **2020**, 67, pp. 8868-8877.

12 Khalifeh, R.; Yasri, M.; Lescop, B.; Gallée, F.; Diler, E.; Thierry, D.; Rioual, S. Development of wireless and passive corrosion sensors for material degradation monitoring in coastal zones and immersed environment. *IEEE J. Ocean.* **2016**, 41, pp. 776-782.

13 Yasri, M.; Lescop, B.; Diler, E.; Gallée, F.; Thierry, D.; Rioual, S. Monitoring uniform and localised corrosion by a radiofrequency sensing method. *Sensors and Actuators B : Chemical* **2018**, 257, pp. 988-992.

14 Khalifeh, R.; Lescop, B.; Gallée, F.; Rioual, S. Development of a Radio Frequency resonator for monitoring water diffusion in organic coatings. *Sens. Actuators A: Phys.* **2016**, 247, pp. 30-36.

15 Sunny, A.I.; Tian, G.Y. Low frequency (LF) RFID sensors and selective transient feature extraction for corrosion characterization. *Sensors and Actuators A: Physical* **2016**, 241, pp. 34-43.

16 Sunny, A.I.; Zhang, J.; Tian, G.Y.; Tang, C.; Rafique, W.; Zhao, A.; Fan, M. Temperature independent defect monitoring using passive wireless RFID sensing system. *IEEE Sensors Journal* **2019**, 19, pp. 1525-1532, 2019.

17 Zhang J.; Tian, G.Y. UHF RFID Tag Antenna-Based Sensing for Corrosion Detection & Characterization Using Principal Component Analysis. *IEEE Trans. Antennas Propag.* **2016**, 64, pp. 4405–4414.

18 Soodmand, S.; Zhao, A.; Tian, G.Y. UHF RFID system for wirelessly detection of corrosion based on resonance frequency shift in forward interrogation power. *IET Microw. Antennas Propag*. **2018** , 12, pp. 1877-1884, 2018.

19 El Masri, I.; Lescop, B.; Talbot, P.; Nguyen Vien, G.; Becker, J.; Thierry, D.; Rioual, S. Development of a RFID sensitive tag dedicated to the monitoring of the environmental corrosiveness for indoor applications. *Sensors and Actuators B: Chemical* **2020**, 322, 128602.

20 Bouzaffour, K.; Lescop, B.; Gallée, F.; Talbot, P.; Rioual, S. Development of an embedded UHF-RFID corrosion sensor for monitoring corrosion of steel in concrete. *IEEE Sensors Journal* **2021**, 21, pp. 12306-12312.

21 Hocker, E.; Almkvist, G.; Sahlstedt, M. The *Vasa* experience with polyethylene glycol: A conservator's perspective. *Journal of Cultural Heritage* **2012**, 13, pp. S175-S182.

22 Taglieri, G.; Daniele, V.; Macera, L.; Schweins, R.; Zorzi, S.; Capron, M.; Chaumat, G.; Mondelli, C. Sustainable Nanotechnologies for Curative and Preventive Wood Deacidification Treatments: An Eco-Friendly and Innovative Approach. *Nanomaterials* **2020**, 10, 1744.

23 Feng, J.; Tian, H.; Huang, Y.; Ding, Z.; Yin, Z. Pyrite oxidation mechanisms in aqueous medium. *Journal of the Chinese chemistry society* **2019**, 66, pp. 345-354.

24 Chandra, A.P.; Gerson, A.R. The mechanisms of pyrite oxidation and leaching: a fundamental perspective. *Surf. Science reports* **2010**, 65, pp. 293-315

25 Jerz, J.K.; Rimstidt, J.D. Pyrite oxidation in moist air. *Geochimica and Cosmochimica Acta* **2004**, 68, pp. 701-714.

26 Perdicakis, M.; Geoffroy, S.; Grosselin, N; Bressière, J. Application of the scanning reference electrode technique to evidence the corrosion of a natural conducting mineral: pyrite. Inhibiting role of thymol. *Electrochimica Acta* **2001**, 47, pp. 211-216.

27 Smith, G.D.; Clark, R.J.H. The role of H_2S in pigment blackening. *Journal of Cultural Heritage* **2002**, 3, pp. 101-105.

28 Coccato, A; Moens, L; Vandenabeele, P. On the stability of mediaeval inorganic pigments: a literature review of the effect of climate, material selection, biological activity, analysis and conservation treatments. *Heritage Science* **2017** , *5, 12.*

29 Canosa, E.; Norrehed, S. Strategies for Pollutant Monitoring in Museum Environments. Swedish National Heritage Board **2019**, Available from: http://rgdoi.net/10.13140/RG.2.2.24172.00640.

30 Barclay, R.L.; Dignard, C.; Selwyn, M. Caring for metal objects. Canadian Conservation Institute **2020**, http://www.publications.gc.ca/site/fra/9.888183/publication.html

31 Sease, C.; Selwyn, L. S.; Zubiate, S.; Bowers, D. F.; Atkins, D. R. Problems with coated silver: whisker formation and possible filiform corrosion. *Studies in Conservation* **1997**, 42, pp.1–10.

 doi:10.20944/preprints202105.0173.v1

32 Ali Ehsan, M.; Khaledi, H.; Ali Tahir, A.; Nay Ming, H.; K.G. Upul Wijayantha, K.G.; Mazhar, M. Synthesis and characterization of silver diethyldithiocarbamate cluster for the deposition of acanthite (Ag_2S) thin films for photoelectrochemical applications. *Thin Solid Film* **2013**, 536, pp. 124-129.

33 Volpe, L.; Peterson, P.J. The atmospheric sulfidation of silver in a tubular corrosion reactor. *Corrosion Science* **1989**, 29 pp. 1189-1196.

34 Pope, D.; Gibbens, H.R.; Moss, R.L. The tarnishing of Ag at naturally-occuring H_2S and SO_2 levels. *Corrosion Science* **1968**, 8, pp. 883-887.

35 Franey, J.P; Kammlot, G.W.; Graedel, T.E. The corrosion of silver by atmospheric sulfurous gases. *Corrosion Science* **1985**, 25, pp. 133-143.

36 R. Bauer, R. Sulfide corrosion of silver contacts during satellite storage. *Engineering Notes* **1988**, 25, pp. 439-441.

37 Conyers Jr., J.L.; White, H.S. Electrochemical growth of Ag_2S on Ag(111) electrodes. Coulometric and X-ray photoelectron spectroscopic analysis of the stepwise formation of the first and second monolayers of Ag_2S. *Journal of Physical Chemistry B* **1999**, 103, pp. 1960-1965.